ESTEC/CONTRACT 8125/88/NL/FG
PRF 141315

Modelling of the MELiSSA artificial ecosystem

Toward a structured model of the nitrifying compartment

- Description of the respiratory chain of nitrifying organisms
- Development of assumptions for the reverse electron flow in the respiratory electron transport chain
- Stoichiometric description of the nitrification
- Determination of K_{La} for oxygen transfer limitation

TECHNICAL NOTE 23.2

L. Poughon
Laboratoire de Génie Chimique Biologique 63177 AUBIERE Cedex, FRANCE

April 1995

T.N. 23.2: Modelling of the MELiSSA artificial ecosystem
TOWARD A STRUCTURED MODEL OF THE NITRIFYING COMPARTMENT

L. Poughon.
Laboratoire de Génie Chimique Biologique
63177 AUBIERE Cedex. France.

INTRODUCTION

In the MELiSSA loop the nitrifying compartment has the same function than the nitrifying process in the terrestrial ecosystem (figure 1) which is to provide an edible N-source for plants or micro-organisms (as Spirulines in the case of the MELiSSA loop). The ammonification processes from organic waste (as for example the human waste faeces and urea) are performed in the MELiSSA loop by the 2 first compartments (liquefying and anoxygenic phototrophs compartments). It must be noted that there are some structural differences between the MELiSSA N-loop and the terrestrial ecosystem:

1- the MELiSSA loop represent a very simplified part of the N loop encountered on earth;
2- the denitrification process (N mineral -> N_2) or the N_2 removing (N_2 -> N mineral) are not considered
3- the sole N - source is NO_3^- for Spirulina, it is NH_4^+ for phototrophs and it is organic N for the crew.

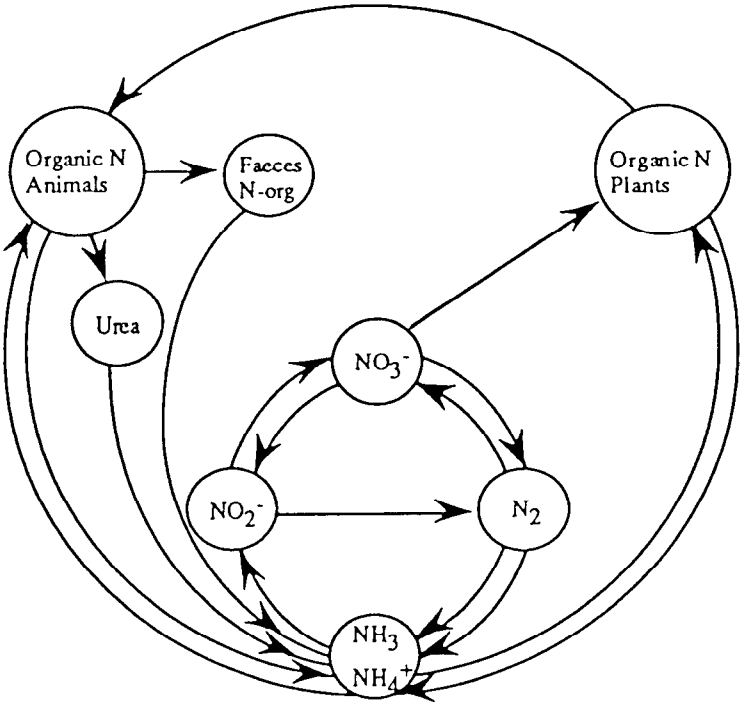

Figure 1: The terrestrial N-cycle.

The 2 last particularities of the MELiSSA loop working are important to outline here, and confirm that the MELiSSA loop is a simplified model for N recycling.

The study of the nitrifying process at the ESA/ESTEC has led to interesting results about the nitrifying performances, the culture working conditions and the processes design . A summary

of the state of art of the fixed bed pilot reactor for nitrification have been reported by Forler (1994).

This note is an extension of the chapter 5 of this report ('energetic metabolism'). Its aims is to present the building of a structured stoichiometry for the nitrification process. The final goal is to achieve an integrated model of the nitrifying compartment including kinetic and stoichiometric data as well as mass transfer requirements..

I - THE MODELLING APPROACHES OF A BIO-PROCESS

It must be kept in mind that the parameters taken into account in order to build a mathematical model of a biotechnological process can be classified in 4 categories (Noorman, 1991):

1- kinetics, quantifying the rate of the biological conversion process;
2- stoichiometry, giving the interdependency of the conversion rates of the different process compounds;
3- hydrodynamics, representing the physical phenomena of mass and heat transfer;
4- economics

The development of correlations for the design parameters can be approach in a number of ways depending on the level of complexity that is needed (figure 2)

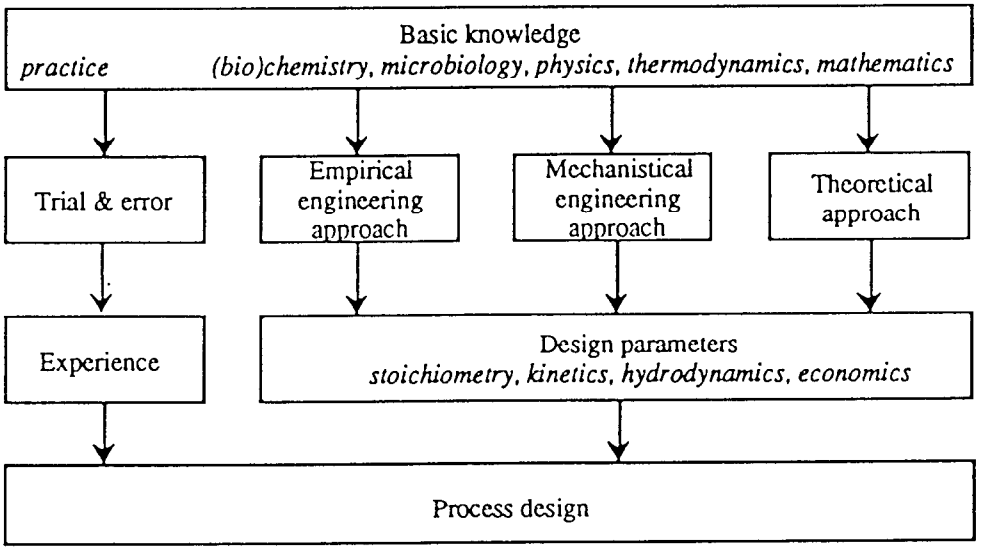

Figure 2: The processes modelling approaches (from Noorman, 1991).

The mechanistical engineering approach (Noorman, 1991) is an attractive compromise between the empirical engineering approach use in industry and the fundamental approach. Here, the basic mechanisms of microbial activity and transport phenomena are taken into account, but the description is limited to the essential features of the process and simplified into manageable form.

Because the biotechnological processes are very complex, especially if they are carried out on the large scale, it is impossible to investigate the different parameter categories simultaneously. Instead, a systematic procedure must be preferred, where kinetics,

stoichiometry and hydrodynamics are treated separately. An example of the mechanistic engineering is given in figure 3.

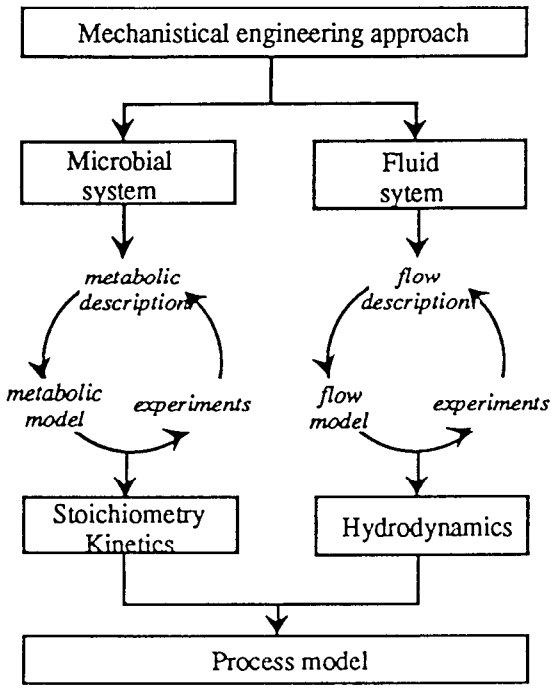

Figure 3: Mechanistical engineering approach (from Noorman, 1991).

The value of such mechanistic models is the possibility to use it, with care, for prediction beyond the experimental boundaries where it is validate.

The models for nitrification presented in the literature are mainly dynamic models involving kinetics and transfer limitation for the substrates. A recent example is the model developed by Hunik et al. (1994). In such models, the nitrification is described using 2 equations:

$$NH_4^+ + 1.5\ O_2 \longrightarrow NO_2^- + 2\ H^+$$

$$NO_2^- + 0.5\ O_2 \longrightarrow NO_3^-$$

A metabolically structured model has been developed by Geraats et al. (1990) for the nitrification and denitrification by *Thiosphaera partotropha*, on which kinetics and diffusion equations were added by Hooijman et al. (1990) for the modelling of oxygen profiles in an immobilised cells reactor.

Our aim for the nitrification process modelling is, as described in figure 3:

- first, the building of a structured stoichiometry for Nitrosomonas and Nitrobacter;
- second, the addition, to this stoichiometry, of a dynamic model similar to the one developed by Hunik et al. (1994).

This note will deal with the first step of the study, *i.e.* the building of a stoichiometry for the nitrification.

II - STRUCTURED STOICHIOMETRIC MODEL FOR THE NITRIFICATION

The term nitrification is defined as the biological conversion of reduced forms of nitrogen to nitrite and nitrate. Two different types of nitrification must be distinguished:

- the lithoautotrophic nitrification. Two groups, ammonia and nitrite oxidisers, are involved, which are characterised by the fact that the inorganic substrates serve as energy sources for growth.
- the heterotrophic nitrification. It is carried out by diverse bacteria or fungi and nitrification is only a cooxydation not coupled with energy generation.

It must be kept in mind that the lithoautotrophic nitrifiers are the only group of organisms producing high amount of nitrite and nitrate from ammonia. There are these lithoautotrophic nitrifiers which are involved in the MELiSSA loop, in which the nitrifying compartment consist of an axenic fixed bed co-culture of *Nitrosomonas europea* and *Nitrobacter winogradsky*.

2.1 - Studies of the nitrification phenomenum

The first studies of the nitrification phenomenum were done by Winogradsky in 1888. He has shown that the nitrification occurs through 2 steps:

- the first is the oxidation of NH_3 to NO_2^- by ammonia oxidisers as *Nitrosomonas sp.*
- the second is the oxidation of NO_2^- to NO_3^- by nitrite oxidisers as *Nitrobacter sp.*

Calorimetric and thermodynamic studies have been performed and a $\Delta G'$ of 17 KJ/mol has been determined for the following reaction (Prosser, 1986):

$$NH_4^+ + \frac{1}{2}O_2 \rightleftharpoons NH_2OH + H^+$$

In this reaction appears the hydroxylamine (NH_2OH), as a go-between in the NH_3 oxidation. The reaction is endergonic, thus it can not lead to ATP production, but the next reaction (hydroxylamine -> nitrite) provides -276.1 KJ/mole of NH_4^+ oxidised.

For the oxidation of nitrate by *Nitrobacter sp.*, the following reaction is proposed, providing a $\Delta G'$ of -73.2 KJ/mol:

$$NO_2^- + \frac{1}{2}O_2 \rightleftharpoons NO_3^-$$

Fenckel and Blackburn.(1979), assuming that only 50% of the energy provided by the oxidations can be used for ATP synthesis, determined that , Nitrosomonas generates 1 to 4% (Nitrobacter 3 to 10%) of the cell material that might be expected by from an heterotroph with the same amoount of available energy..

2.1.1 Ammonia oxidation

The Ammonia Mono Oxygenase (AMO)

The first stage in ammonia oxidation is its conversion to hydroxylamine. This reaction is carried out by a membrane bound ammonia monooxygenase for which the substrate is ammonia

(NH_3) rather than the ammonium ion (NH_4^+) (Suzuki et al., 1974). The reaction is endergonic ($\Delta G' = +17$KJ/mol) and thus can not produce ATP.

The ammonia monooxygenase is appearing as a useful enzyme for oxidation reactions and had been the subject of many studies, especially for its ability to oxidise low molar weight organic compound. For the monooxygenase, Wood (in Prosser 1986) had proposed a speculative catalytic cycle, based upon the one for tyrosinase (figure 4). This cycle involves molecular oxygen as an oxygen source and a source of reducing power.

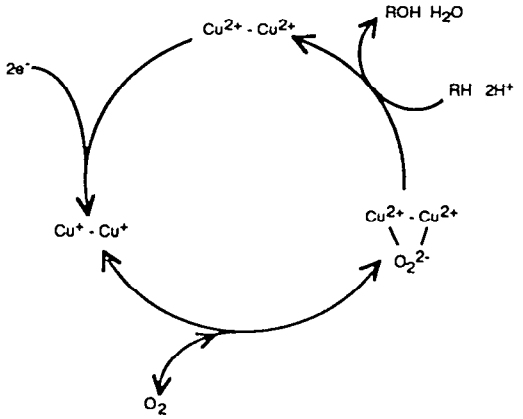

Figure 4: catalytic cycle of tyrosinase.

For uncharged ammonia as substrate (nitrification), the monooxygenase reaction is then:

$$NH_3 + O_2 + 2\,H^+ + 2\,e^- \rightleftarrows NH_2OH + H_2O$$

The enzyme can in principle accept electrons from everywhere in the respiratory chain (Wood, 1986), and Wood suggested that the monooxygenase accept electrons from the Ubiquinone -cytochrome b region- of the electron transport chain. It must be noted that $NADH,H^+$ can work as an electron donor and is then the priming agent in isolated membrane (Tsang and Susuki, 1982). It is not known whether the proton oxidation of ammonia occurs on the cytoplasmic or periplasmic side of the membrane.

The Hydroxyl-Amine Oxydo-reductase (HAO)

The second stage of ammonia oxidation is the conversion of hydroxylamine to nitrite. This four electron oxidation needs the introduction of a second oxygen, coming from water (Anderson and Hoopper, 1983), implying enzymatic and non enzymatic reactions, such as:

$$E + NH_2OH \longrightarrow E-NHO + 2\,H^+ + 2\,e^-$$
$$E-NHO \longrightarrow E-NO + H^+ + e^-$$
$$E-NO \longrightarrow E-NO^+ + e^-$$
$$E-NO^+ + H_2O \longrightarrow E + HNO_2 + H^+$$

$$NH_2OH + H_2O \xrightarrow{[HAO]} NO_2^- + 4\,e^- + 5\,H^+$$

The hydroxylamine oxidation is brought about by hydroxylamine oxidoreductase (HAO), which has been located in the periplasm (Olson and Hooper,1983).

The pathway of the four electrons involved in the HAO reactions is not clear. Electrons are thought to flow from the hydroxylamine to c-haemes of HAO and then probably through an "electron exit" to the soluble cytochrome c_{554} located in the periplasm. Then, via a cytochrome c_{552}, the electrons can reach the terminal oxidase (cyt a_1) of the respiratory chain. Thus the path of the electrons from hydroxylamine could be:

$$NH_2OH \longrightarrow HAO \longrightarrow \text{cyt } c_{554} \longrightarrow \text{cyt } c_{552} \longrightarrow \text{terminal oxydase}$$

Wood (1986) integrated an Ubiquinone-Cyt b/c complex of the respiratory chain in this pathway, what may possible a proton motive Q-cycle (see section 2.3). The integration of this complex raises the problem of the electron path. Different schemes were proposed (figure 5):

- first, it can be supposed that the four electron feed the Ubiquinone complex;

- second, Wood (1986) noted that because hydroxylamine oxidation is an irreversible process, the reaction must loose energy as heat, implying release of electrons at a higher potential than for thermodynamic equilibrium. But the redox potential for hydroxylamine oxidation (+60 mV) is essentially the same as the Ubiquinone reduction to Ubihydroquinone (+90 mV). Thus, it can be assumed that three electrons from hydroxylamine reach the main chain at Ubiquinone, while the fourth is treated separately and joins it at the Class I cytochrome c;

- a third description can be made, involving each step of the hydroxylamine oxidation. In that case, 2 electrons feed hydroxylamine while the two other are released at a lower potential.

Consequently, the respiratory chain is branched with ammonia monooxygenase and the terminal oxydase competing for electron and the control of the electron flow occurs through 2 mechanisms:

- the electron flow to the terminal oxydase which may be restricted by the protomotive force;
- the hydroxylamine which inhibits the ammonia monooxygenase, providing a feed back inhibition mechanism with the establishment of a low steady state concentration of hydroxylamine.

However, as shown in figure 5, it must be kept in mind that 2 electrons from the hydroxylamine oxidation are used to feed the AMO.

2.1.2 Nitrite oxidation

The nitrite oxidation to nitrate occurs without detectable intermediates, and is carried out by the soluble nitrite oxidase enzyme. The extra oxygen atom in nitrate is derived from water (Aleem et al, 1965):

$$NO_2^- + H_2O \xleftrightarrow{[E]} NO_3^- + 2H^+ + 2e^-$$

The enzyme (E) can work reversibly, and it can anaerobically carry out the reduction of nitrate (Aleem and Sewell, 1984). This reversibility implies that the enzyme redox centres must have a potential close to that of the nitrate-nitrite couple (E'_0=+430 mV). It is generally assumed that the reaction of the membrane bound deshydrogenase occurs in the cytoplasmic side and that the electrons are transmitted to the cytochrome c of the respiratory chain.

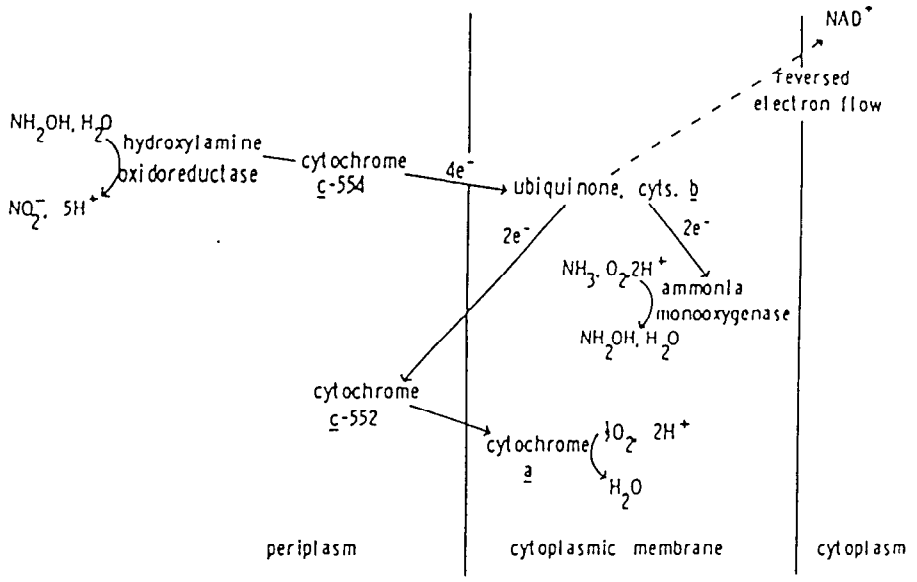

Figure 5-a
(from Wood, 1986)

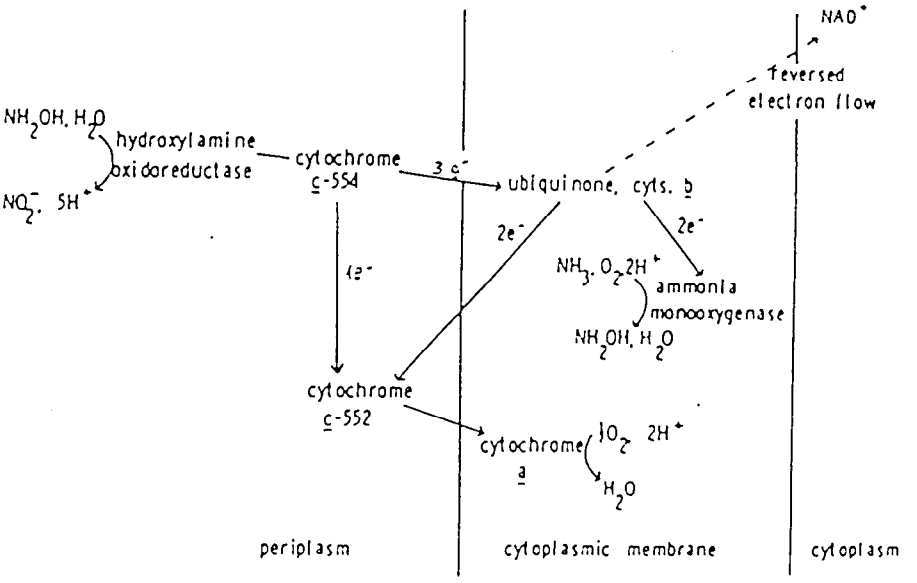

Figure 5-b
(modified from Wood, 1986)

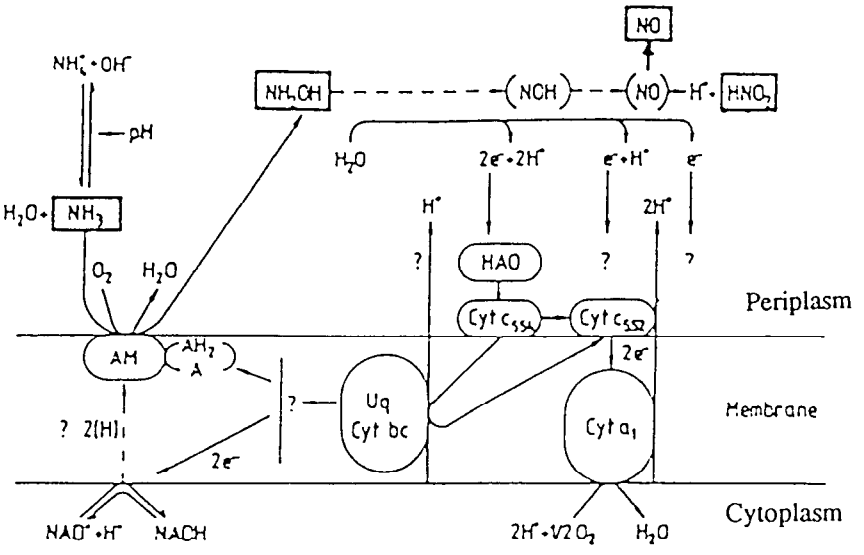

Figure 5-c
(from Bock et al., 1991)

Figures 5: schemes of different hypothetical models for electron transport in ammonia oxidation

Coupling of nitrite oxidation to the generation of a protomotive force is theoretically possible, but the detailed mechanism has yet to be elucidated. Wood (1986) discussed the experimental evidence for mechanism of energy generation by nitrite oxidation (see section 2.3) and proposed the scheme illustrated in figure 6.

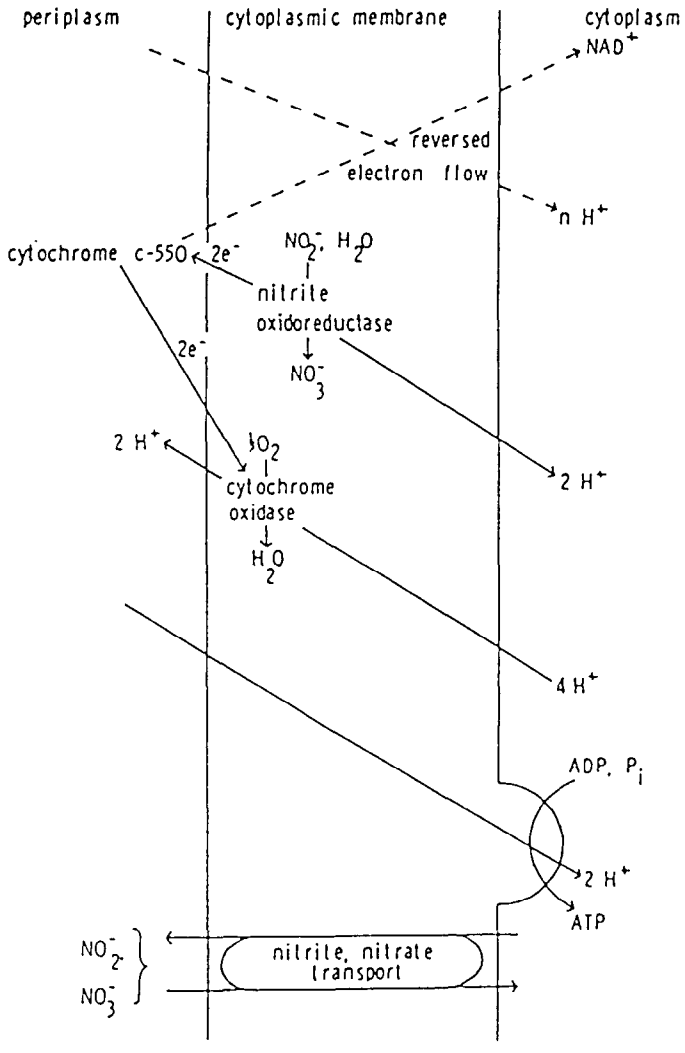

Figure 6: Nitrite oxidation and energy generation (from Wood, 1986).

2.2 - Carbon metabolism

The major source of carbon for nitrifying bacteria is carbon dioxide which is fixed via the Calvin cycle (figure 7). In some strains, only soluble RuBisCo is found, while other have both soluble enzyme and carboxysome-bound RuBisCo.

The NO_2^-/NH_4^+ redox potential is + 340 mV and that for NO_3^-/NO_2^- is +430 mV. These potentials are vastly more positive than the $NAD^+/NADH,H^+$ couple, and indeed, ammonia and nitrite are at the limit for provision of energy for growth. The Calvin Cycle requires high source of reduced power (figure 7). Thus, a way for reducing power synthesis is needed. An energy-driven reversed electron flow is then necessary to reduce NAD^+ (figures 5 and 6) (Prosser, 1989). The reverse electron flow in the respiratory chain is assumed to be driven by a

proton flow from the periplasmic (out) to the cytoplasmic (in) side of the membrane, what can be summarised, in the case of Nitrobacter, by the following equation:

$$2\ \text{cyt c}\ (Fe^{2+}) + NAD^{+} + N\ (H^{+}_{out}) \longrightarrow 2\ \text{cyt c}\ (Fe^{3+}) + NADH,H^{+} + (N-2)\ (H^{+}_{in})$$

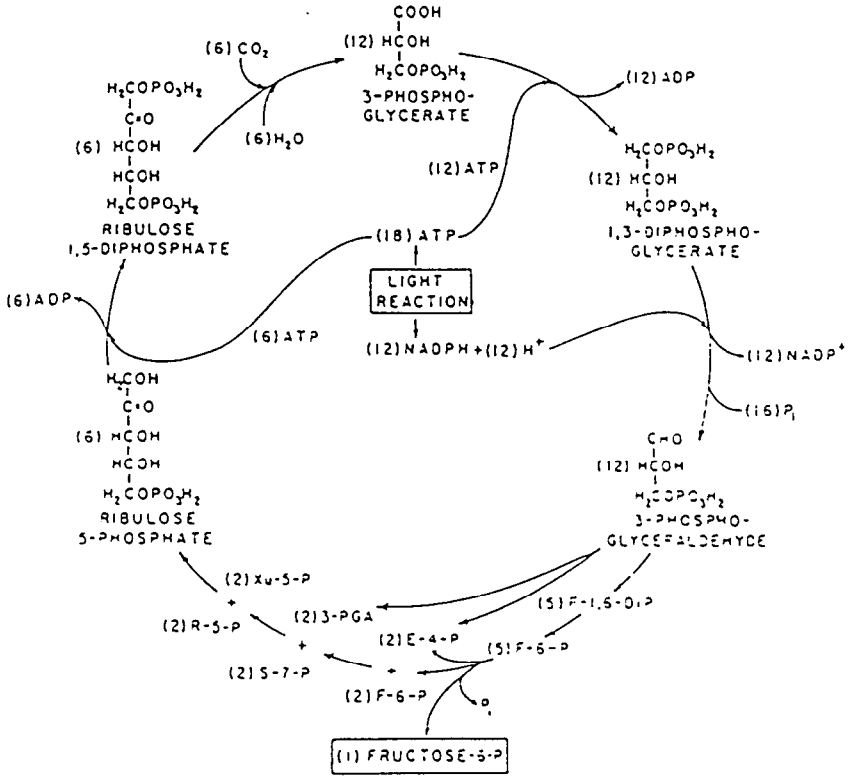

Figure 7: the Calvin-Benson cycle.

As a consequence of this energy-driven reversed electron flow, much of the limited amount of energy generated by ammonia and nitrite oxidation is therefore used to generate reduced power.

On thermodynamic ground, Kelly (1928) has estimated that 80 % of energy generated by autotrophs is used to fix CO_2, and Glover (1985) determined thermodynamic efficiencies for growth in the range of 4.4-21.3%. Consequently, a small amount of biomass turn over a very large amount of ammonia (Fenckel and Blackburn, 1979), *i.e.* a small amount of biomass is generated by the oxidation of ammonia (tables 1 and 2)

Table 1: Relation ship between ammonia oxidised and carbon dioxide assimilated (taken from Gunsalus and Stanier, 1962)

	Culture number			
	11	12	26	30
Ammonia N oxidised (mg)	722	506.1	928.3	815.4
Carbon assimilated (mg)	19.7	15.2	26.4	22.4
Ammonia N oxidised/Carbon assimilated	36.6	33.3	35.2	36.4

It must be noted that the assimilation of organic compounds by ammonia oxidisers has been studied (positives or negatives effects on the growth of different species in presence of amino-acids or organic acids). If heterotrophic growth (organic compound as carbon and energy

source) has never been observed, the mixotrophic growth of ammonia increased the yield of biomass formed per unit of ammonia converted.

For nitrite oxidisers, heterotrophic growth has been demonstrated and mixotrophic growth stimulates both cell yield and maximum specific growth yield.

Table 2: Yield and maintenance coefficients for nitrifying bacteria (taken from Prosser, 1989)

Ammonia oxidizers	
Biomass and cell yield on ammonia:	
Nitrosomonas sp.	0.42–1.40 g biomass mol^{-1}
Nitrosomonas europaea	0.6–0.8 g biomass mol^{-1}
Nitrosomonas europaea	1.26–1.72 g biomass mol^{-1}
Nitrosomonas ATCC	$4.61–6.44 \times 10^{12}$ cells mol^{-1}
Nitrosomonas FH1	$1.38–2.44 \times 10^{12}$ cells mol^{-1}
Nitrosospira sp.	$8.04–10.6 \times 10^{12}$ cells mol^{-1}
Nitrosolobus sp.	$1.85–2.24 \times 10^{12}$ cells mol^{-1}
True growth yield	5.88 g biomass mol^{-1}
Maintenance coefficient	0.88 mol g $biomass^{-1}$ h^{-1}
Carbon yield on ammonia (ratio of CO_2 fixed: NO_2^- produced):	
Nitrosomonas sp.	0.090
Nitrosomonas sp.	0.033
Nitrosomonas spp.	0.081–0.094
Nitrosomonas marina	0.04–0.07
Nitrosospira spp.	0.075–0.096
Nitrosocystis oceanus	0.07–0.13
Nitrosocystis oceanus	0.06–0.10
Nitrosococcus mobilis	0.014–0.031
Nitrite oxidizers	
Biomass yield on nitrite:	
Nitrobacter sp.	1.11–1.51 g biomass mol^{-1}
Carbon yield on nitrite (ratio of CO_2 fixed: NO_3^- produced):	
Nitrobacter sp.	0.013–0.014
Nitrobacter sp.	0.0125
Nitrobacter sp.	0.02
Nitrobacter spp.	0.02–0.03
Nitrococcus mobilis	0.014–0.031
True growth yield	9.8 g biomass mol^{-1}
Maintenance coefficient	0.78 mol $biomass^{-1}$ h^{-1}

The central metabolic pathways have been studied. It has been shown that the α-ketoglutarate deshydrogenase is present in heterotrophic growth of Nitrobacter, but not in autotrophic growth, what is in keeping with the hypothesis that the presence of α-ketoglutarate deshydrogenase is not compatible with a carbon economy based on CO_2 fixation by the requiring-energy RuBP carboxylase pathway (Bock et al., 1991).

2.3 - Electron transfer, protomotive force, ATP synthesis and $NADH,H^+$ synthesis

The ATP and $NADH,H^+$ synthesis occur by electrons transport and the proton gradient generation due to the working of the respiratory chain, linked to the ammonia (or nitrite) oxidation. Although the interrelations between ammonia (or nitrite) oxidation, transfer of electrons and respiratory chain working had been studied, many assumptions and unknowns already stay, especially about the reverse electron flow for the $NADH,H^+$ synthesis.

In order to built a complete (but hypothetical) representation of the ATP synthesis, $NADH,H^+$ synthesis, electron transport and proton gradient generation for the lithoautotrophic nitrifiers, a short description of the classical mitochondrial respiratory chain is appeared

necessary (see section 2.3.1). From this basic knowledge, and assuming the present assumptions about electrons transfer in ammonia (see section 2.1 and 2.3.2) and nitrite (see section 2.2 and 2.3.3) oxidation, a complete theoritical energy metabolism of the two organisms can be built.

2.3.1 The mitochondrial respiratory chain

This section describe the functioning of a classic mitochondrial respiratory chain. That will present the basis of oxidative phosphorylation, which is important in many genera of bacteria (but not of course in organisms that exist by fermentation alone).

The bacterial oxidative phosphorylation is a very large topic, not only because there are many different sources and acceptors of electrons, but also because the compounds involved in electron transfer can differ markedly between the organisms or within a same genus, depending on growth conditions.

As mentioned above, only a part of the electron transfer chain of lithoautotrophic nitrifiers is known. Assuming that the unknown part functions as a classical mitochondrial respiratory chain, the knowledge of this chain would lead to a complete description of this chain in lithoautotrophic nitrifiers.

Description of the mitochondrial respiratory chain

The electron transfer in the respiratory chain occurs through a succession of oxidoreduction reactions involving low variation of oxidoreduction potential for each step (table 3 and figure 8). The reactions are carried out by deshydrogenases, Fe-S proteins, Ubiquinone and cytochromes (class a, b, c, d or o) (figure 9). Experimentally and by thermodynamic calculations, 4 sites of energy conservation (complexes) have been determined among the mitochondrial respiratory chain (figure 9).

Table 3: Mid point potential of some compounds involved in the respiratory chain and some redox couples able to act on the respiratory chain (taken from Nicholls and Ferguson, 1992).

$ox + ne^- + mH^+ = red$				
	n	m	$E_{m,7}$ (mV)	Change in E_m (mV) when pH increased by 1 unit
Methyl viologen ox/red	1	0	−450	0
Ferredoxin ox/red	1	0	−430	0
$H^+/\frac{1}{2}H_2$ (H_2 1 atm)	1	1	−420	−60
NAD^+/NADH	2	1	−320	−30
$NADP^+$/NADPH	2	1	−320	−30
Menaquionone/menaquinol	2	2	−74	−60
Fumarate/succinate	2	2	+30	−60
Ubiquinone/ubiquinol	2	2	+40	−60
Ascorbate ox/red	2	1	+60	−30
PMS ox/red	2	1	+80	−30
Cyt *c* ox/red	1	0	+220	0
DCPIP/$DCPIPH_2$	2	2	+220	−60
DAD/$DADH_2$	2	2	+275	−60
TMPD ox/red	1	0	+260	0
Ferricyanide ox/red	1	0	+420	0
O_2(1 atm)/$2H_2O$ (55 M)	4	4	+820	−60

DAD is 2,3,5,6-tetramethylphenylene diamine; PMS is phenazine methosulphate; TPMD is *N,N,N',N'*-tetramethyl-*p*-phenylene diamine; DCPIP is 2,6-dichlorophenolindophenol.

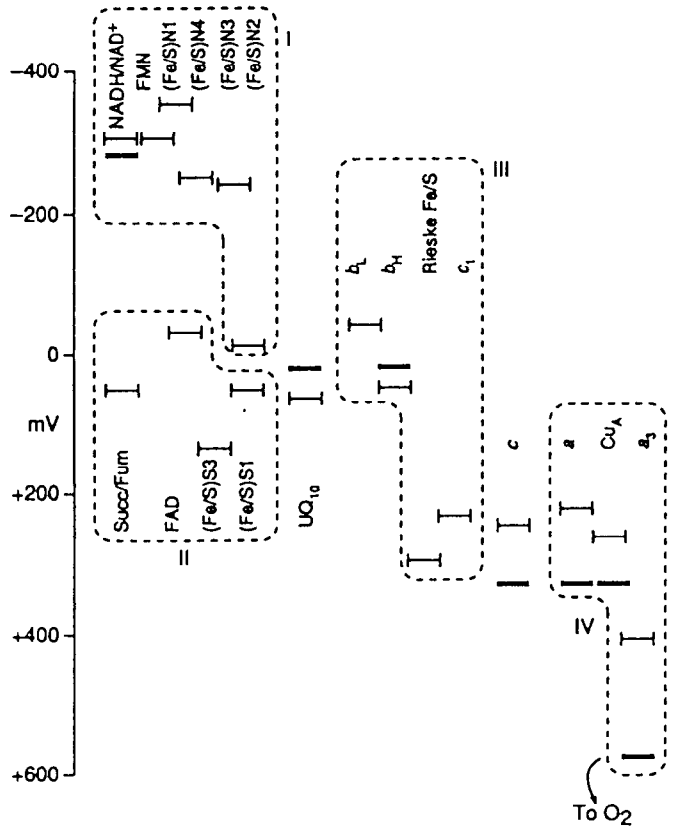

Figure 8: $E_{m,7}$ values (mid potential at pH 7) for components of the mammalian mitochondrial respiratory chain, and $E_{h,7}$ values (potential for mitochondria respiring in state 4 at pH 7).taken from Nicholls and Ferguson, 1992.

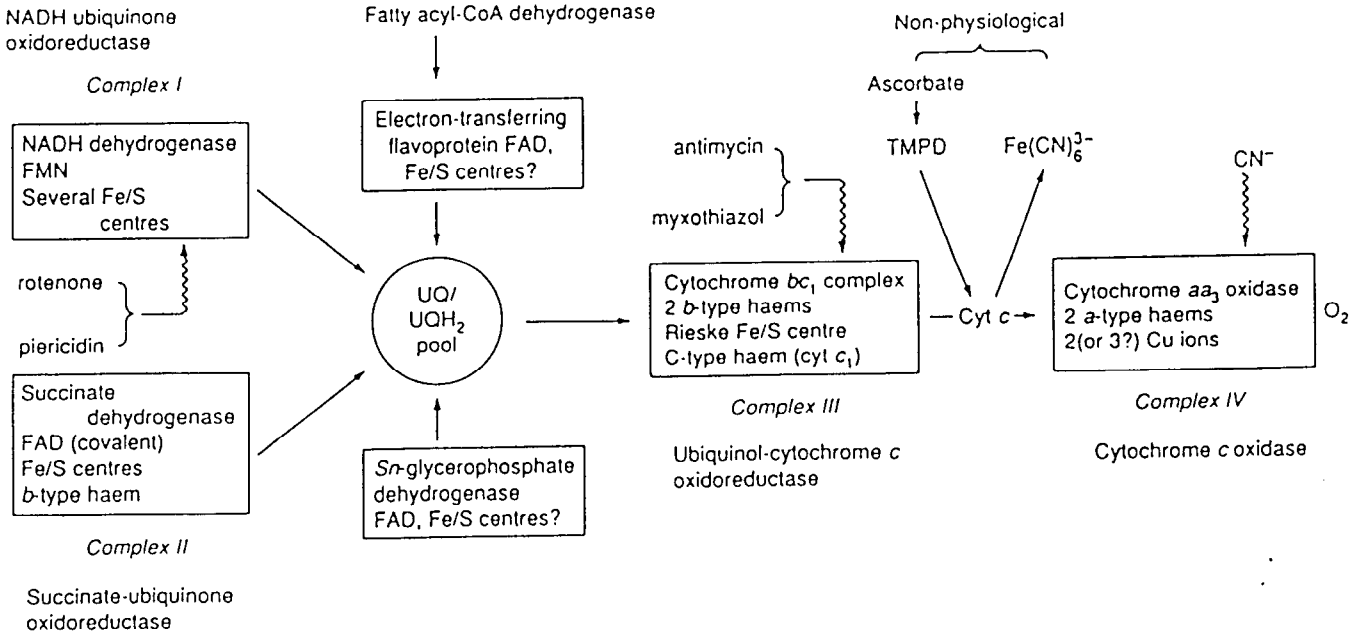

Figure 9: An overview of the redox carrier in the mitochondrial respiratory chain and their relation to the four respiratory chain complexes. Arrows indicate site of action of an inhibitor.

The function of the respiratory chain is to transfer electrons through a redox potential span of 1.1 V of $NAD^+/NADH,H^+$ couple to the $O_2/2H_2O$ couple. Much of the chain is reversible, but it must be kept in mind that the terminal oxidase (complex IV) is an irreversible process.

Electron transfer, proton motive force and ATP synthesis: the chemiosmotic theory

According to Mitchell (1967), Δp (the proton motive force) is generated in the respiratory chain of mitochondria as a consequence of alternation of transmembrane H^+ transfer by diffusible hydrogen carrier and electron transfer by cytochromes or Fe-S proteins. The chemiosmotic theory is based upon the assumption of the impermeability of the intern membrane of mitochondria to H^+. The oxidoreduction reactions of the respiratory chain are then oriented in the wall and act as "proton pumping", driving H^+ from the internal side to the external side, generating a Δp. This protomotive force is further used to promote the ATPase activity and ATP synthesis (figure 10).

Table 4: values for Δp, ΔpH and Δψ, for energy-transducing membranes.(from Nicholls and Ferguson, 1992)

Membrane	Δψ (mV)	ΔpH (units)	Δp (mV)
Liver mitochondria	170[a]	≤0.5[b]	≤200
Submitochondrial particule (heart)	150[c]	≤0.5[d]	≤180
Thylacoids	0[c]	3.3[d]	195
Inside-out vesicles from *P. denitrificans*	160[c]	≤0.5[d]	≤190
E. coli cells at pH 7.5	140[a]	≤0.5[b]	≤170

a From distribution of TPP^+ or $^{86}Rb^+$
b From distribution of acetate or 5,5 dimethyl-oxazolidene 2,4 dione
c From distribution of SCN^- or CLO_4^-
d From distribution of alkylamine

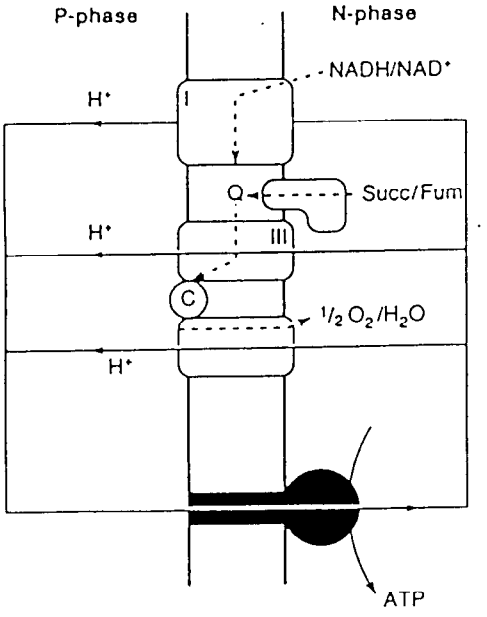

Figure 10: The proton circuit of the chemiosmotic theory. Solid lines: proton flux; dashed lines: electron flow; P phase: cytoplasmic side of mitochondria; N phase: matrix side (taken from Nicholls and Ferguson, 1992).

However, it must be noted that Δp is not the result of the sole proton gradient, but a combination of the ΔpH (proton gradient across the membrane) and of the $\Delta\psi$ (membrane potential). Table 4 (taken from Nicholls and Ferguson, 1992), presents some approximate values for the protomotive force as well as its two components ΔpH and $\Delta\psi$, that have been determined for a number of energy-transducing membranes.

Since the chemiosmotic theory of Mitchell, the proton stoichiometry of mitochondrial complexes ($H^+/2e^-$ ratio) and of the ATP synthesis (H^+/P ratio) have been the subject of many studies. The following description of the complexes and their stoichiometries (Nicholls and Ferguson, 1992) shortly summarises the present representation of the mitochondrial complexes.

Complexes of the mitochondrial respiratory chain

Complex I: NADH-UQ oxidoreductase

It is the least well understood component of the mitochondrial chain. There may be as many as 7 Fe/S centres in the complex, four of which, called N-1, N-2, N-3 and N-4 (figure 11) are well characterised. Using the $E_{m,7}$ values as a guide (but it must be kept in mind that it is the value of Eh that are relevant) a likely pathway of electron flow may be:

$$NADH \longrightarrow FMN \longrightarrow N-1 \longrightarrow N-4 \longrightarrow N-3 \longrightarrow N-2 \longrightarrow UQ$$

There is also tentative evidence for an internal UQ molecule, involved in H^+ translocation but not exchangeable with the bulk of UQ pool, similar to that found in photosynthetic reaction centres.

What is certain about complex I is that it catalyses the transfer of 2 electrons from $NADH,H^+$ to Ubiquinone (UQ_{10} in mitochondria) in a reaction that is associated with proton translocation. A current evidence suggests that the proton translocation stoichiometry is $4H^+/2e^-$, but the mechanism is unknown. Figure 11 is a tentative structure based on evidence from electron microscopic studies, sequence data and the manner in which complex I splits into different modules (UQ_i is a putative internal Ubiquinone).

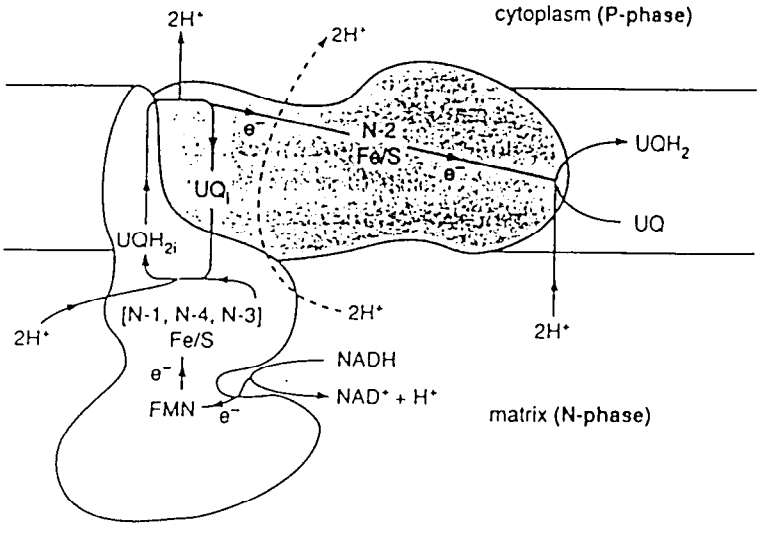

Figure 11: A structure for the mitochondrial NADH-UQ oxidoreductase (from Nicholls and Ferguson, 1992)

Complex II: succinate dehydrogenase.

In addition to complex I, three other redox pathway feed electrons to UQ_{10} (figure 9). Complex II transfers electrons from succinate. The complex consists of several polypeptides (figure 9), and as would be expected on thermodynamic grounds, it is not proton translocating.

Complex III: UQ-cytochrome c oxydoreductase.

The transfer of electrons from ubiquinol to cyt c and the associated proton translocation is not a simple matter. This complex is also found in many bacteria. the probable pathway of electrons through the complex is at first sight convoluted and involved 2 steps (figures 12-a and 12-b).

It must be noted that the complex is truncated in 3 parts:

- an UQ/UQH_2 pool in the membrane. It exists in large molar excess over the other components of the respiratory chain, and can migrate freely in the membrane.
- the binding site Qp (also called Qo or Qz), close to the cytoplasmic side of the mitochondria (or P phase) and adjacent to the Rieske Fe/S protein.
- the binding site Qn (also called Qi or Qc), close to the matrix of mitochondria (or N phase).

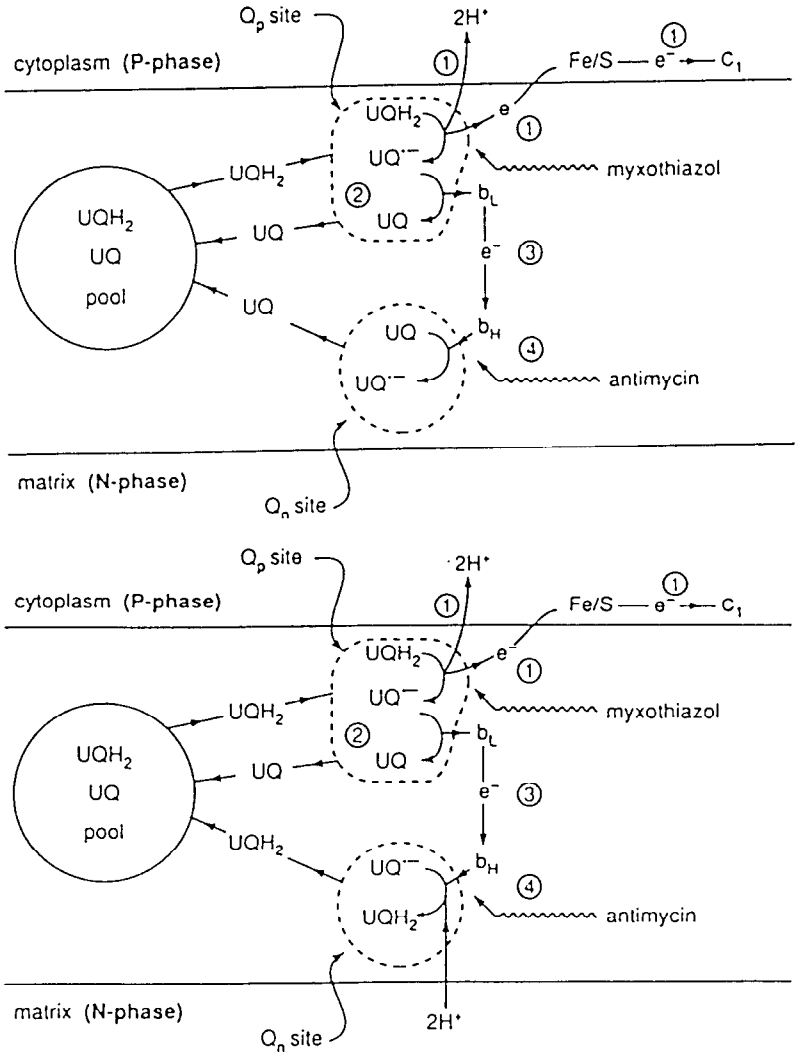

Figures 12-a and 12-b: The Q cycle in mitochondria (from Nicholls and Ferguson, 1992)

How occur the electron transport through these 2 sites and its associated proton translocation (figure 12) ?

The first stage involves 2 steps (steps 1.1 and 1.2).

Step 1.1: UQH2 oxidation at Qp (figure 12-a).
The first electron is transferred from UQH_2 to the Rieske Fe/S protein, releasing 2 protons in the cytoplasm, and leaving the free radical $UQ^{\cdot -}$ at the Qp site. The electron received by the Rieske Fe/S protein passes then down the chain to Cyt c_1 and Cyt c.
The second electron is transferred to the b_L haem close to the P phase.
The reaction is thermodynamically feasible (table 5), implying that the semiquinone is instable and its oxidation is energetically favourable. As a consequence, the one electron oxidation has thus generated a highly reducing electron.

Table 5: $E_{m,7}$ values of the complex III components

Oxidoreduction couple	$E_{m,7}$ (mV)	
$UQH_2/UQ^{\cdot -}$	280 (close to Rieske protein)	1 electron oxidation
UQH_2/UQ	60	2 electrons oxidation
b_H	50	1 electron oxidation
b_L	-100	1 electron oxidation
$UQ^{\cdot -}/UQ$	-160	1 electron oxidation

Step 1.2: UQ reduction to $UQ^{\cdot -}$ at Qn
The transfer of the electron from the bL haem (face P, -100 mV) to the b_H haem (face N, 50 mV) is against the membrane potential (among -160mV). The drop of the electron to a more positive redox (ΔE=150mV) compensated this energetically unfavourable migration.

The Qn site, close to the b_H haem, binds UQ and allows the transfer of the electron from the reduced b_H. The reaction is thermodynamically unlikely since the $UQ^{\cdot -}/UQ$ $E_{m,7}$ value is -160mV, while the b_H $E_{m,7}$ is 50mV. However, assuming a ten fold difference in the binding of the $UQ^{\cdot -}$ relative to UQ, shift $E_{m,7}$ 60mV more positive than if the reaction occurs in free solution. A 300 fold firmer binding of $UQ^{\cdot -}$ would thus make the $E_{m,7}$ 150 mV more positive, allowing the reaction (figure 12-a).

The second step involves, as the first, 2 steps (2.1 and 2.2) and the first of them (step 2.1) is the same as the step 1.1 (see figure 12).

Step 2.2: $UQ^{\cdot -}$ reduction to UQH_2 at Qn
From the b_H haem, a second electron completes the reduction of $UQ^{\cdot -}$ (firmly bound to Qn as supposed in step 1.2) to UQH_2. The 2 protons needed are taken up on the matrix.

To conclude, the functioning of the complex III can be summarised as following:

- 2 electrons are transported from UQH2 to Cyt c
- the two sites involved (Qp and Qn) are not equivalent
- the global stoichiometry is 4 H^+ appearing in cytoplasm by the transport of 2 electrons, while only 2 H^+ disappear in the matrix.

Complex IV: Cyt c - cytochrome oxydase.

It is the final step in the electron transport chain of mitochondria and in certain species of respiratory bacteria operating under aerobic conditions. The cytochrome oxydase catalyses a four electron oxidation from a pool of reduced Cyt c to O_2:

$$O_2 + 4e^- + 4H^+ \longrightarrow 2H_2O$$

In addition to electron transport, the cytochrome oxydase acts as a proton pump with a stoichiometry of $1H^+/1e^-$, but the mechanism of coupling between electron transfer and proton pumping is still unclear (figure 13).

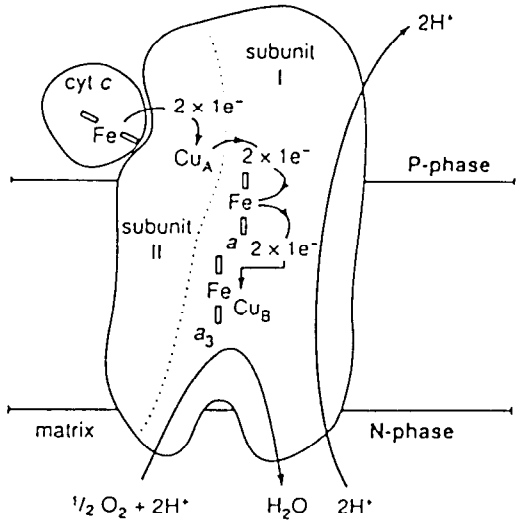

Figure 13: A tentative outline structure for cytochrome oxidase (from Nicholls and Ferguson, 1992).

ATP synthase

The function of the ATP synthase is to utilise Δp to maintain the mass action ratio for the ATPase reaction 7 to 10 orders of magnitude away from the equilibrium or, in case of fermentative bacteria, to utilise ATP to maintain ΔP. The proton translocating ATPase catalyses then a reversible reaction, although its function is the synthesis of ATP rather than hydrolysis.

The purpose of here, is not to give a detailed description of the mechanisms of the ATP synthase, but 3 results must be kept in mind:

- the ATP synthase is highly conserved in the different life forms. It is present in mitochondria, chloroplast and both aerobic and photosynthetic bacteria.
- the balance of experimental evidence suggests an H^+/ATP ratio of 3.
- the reaction carried up by ATP synthase is reversible, i.e., if the translocation of 3 H^+ from the cytoplasmic side of the mitochondria membrane to the matrix drives the synthesis of 1 ATP (H^+/ATP=3), the hydrolysis of 1 ATP will drive the transport of $3H^+$ from the matrix to the cytoplasm (generation of Δp).

Assuming that the respiratory chain of ammonia and nitrite oxidisers has a structure and mechanisms closed to that of the mitochondrial chain, a stoichiometry of the energy and substrate oxidation metabolism can be built. That is the purpose of the two following sections.

2.3.2 Energy metabolism of ammonia oxidisers.

As described in section 2.1.1, 3 schemes (figure 5) are proposed for the mechanism of ammonia oxidation. The second, proposed by Wood (1986), seems to be the most manageable and the most realistic (involving known components), and thus has been chosen.

Assuming the description of the mitochondrial respiratory chain, the proton translocation associated to the electron transport can be added to the figure 5-b. It must be noted that the electrons feeding the UQ pool (from Cyt c_{554}), reduces UQ to UQH_2 by an unclear mechanism. If the following reaction is supposed:

$$\text{Cyt } c_{554} \text{ (reduced pool)} + 2H^+ + UQ \xrightarrow{2e^-} \text{Cyt } c_{554} + UQH_2$$

it could be assumed that the electrons resulting of the hydroxylamine oxidation reach the complex II of the respiratory chain, allowing a Q-cycle (figure 12). The electrons further reach the terminal oxidase through the normal path of the chain. (figure 9).

The problem of reduced power and reverse electron flow has still now to be solved. In other words, how can NAD^+ be reduced from UQH_2 ?

Under certain conditions, the complexes I and III (and never the IV) can run backwards. This supposes an electron donor (other than $NADH,H^+$ on complex I) and the generation of Δp by ATP hydrolysis. Rottenberg and Gutman (1977) have investigated the ATP dependant reverse electron flow from succinate (complex II) to $NADH,H^+$ in bovin heart submitochondrial particules. They indicate an ATP/$2e^-$ ratio of 1.3 (or greater), and suggest that it can be the result of a stoichiometry of $3H^+$/ATP for ATP hydrolysis (see below) and of 4H+/2e- for the span succinate -> NAD.

Thus, these results demonstrate the reversibility of the span UQH_2 -> NAD, which can be written, according to the mitochondria respiratory chain (see section 2.3.1), as:

$$NAD^+ + UQH_2 + 4\ H^+_{\text{cytoplasmic}} \rightleftharpoons NADH,H^+ + UQ + 4\ H^+_{\text{matrix}}$$

Assuming that the mitochondrial and the ammonia oxidisers (*Nitrosomonas sp.*) respiratory chains are close, it is possible to suppose that this reaction carries out the generation of NADH,H+ in ammonia oxidisers.

The complete stoichiometry (electron transport and its associated proton translocation) is reported in figure 14, and can be represented by the following group of reactions.

$$NH_3 + \frac{5}{4}O_2 + 4H^+_{in} + \frac{1}{2}UQ \longrightarrow 4H^+_{out} + (NO_2^-, H^+) + \frac{1}{2}UQH_2 + \frac{1}{2}H_2O$$

$$UQH_2 + 6H^+_{in} + \frac{1}{2}O_2 \longrightarrow UQ + 6H^+_{out} + H_2O$$

$$NAD^+ + UQH_2 + 4H^+_{out} \rightleftarrows NADH,H^+ + UQ + 4H^+_{in}$$

$$3H^+_{out} + ADP + Pi \rightleftarrows 3H^+_{in} + ATP + H_2O$$

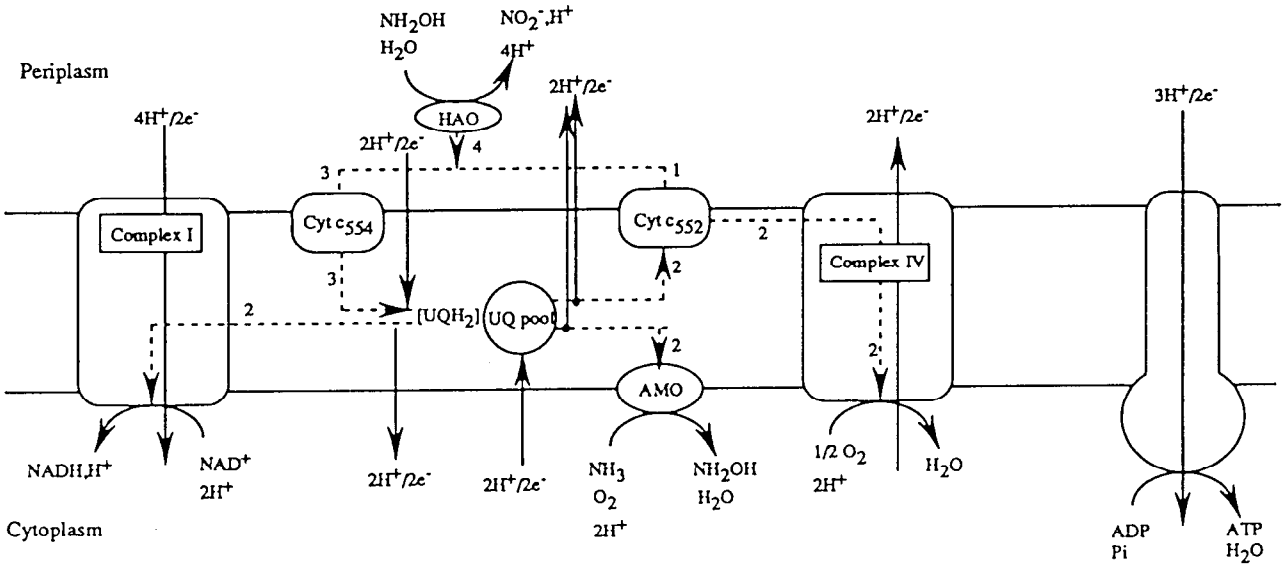

Figure 14: Proposed description of energetic metabolism of ammonia oxidisers

2.3.3 Energy metabolism of nitrite oxidisers.

As described in section 2.1.2, the oxidation of nitrite is a simpler reaction than the ammonia oxidation. However, the mechanism of nitrite oxidation and especially of the Δp generation has not been fully elucidated.

Hooper (1987) presents several models for nitrite oxidation, assuming different configurations for the reaction location (periplasmic or cytoplasmic side), the possibility of proton translocation by nitrite oxidase and the evidence or not of a proton pumping by the cytochrome oxidase.

Figure 15 (from Nicholls and Ferguson, 1992) presents a plausible, but not yet fully proven, scheme in which NO_2^- oxidation occurs in the cytoplasmic side, transferring electrons to cytochrome c (periplasmic side) and then to the terminal proton pumping cytochrome aa_3 oxidase.

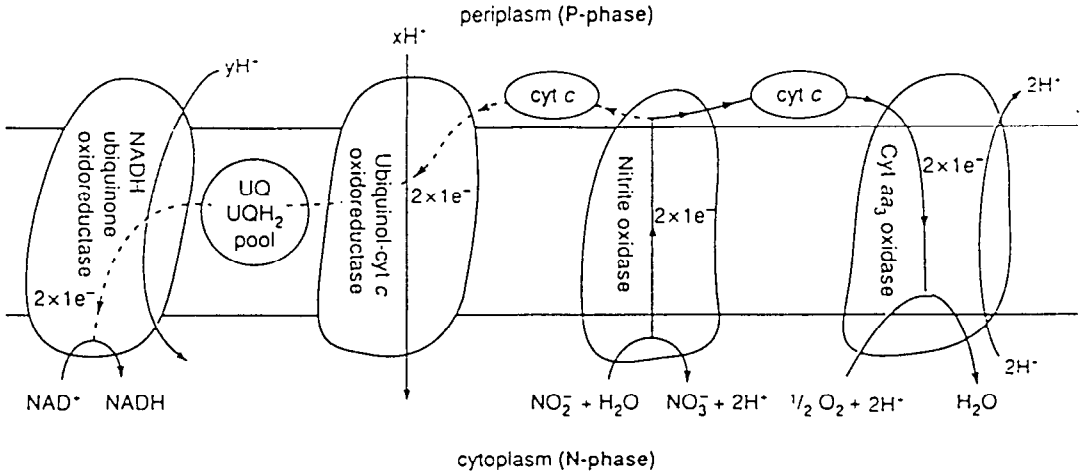

Figure 15: Proton motive force and reversed electron transport in Nitrobacter (from Nicholls and Ferguson, 1992)

The reverse electron flow from Cyt c to NAD^+ is driven through complexes I and III, respectively by a proton translocation of y and x H^+. it can be assumed that y can be set to the value of 4H+, as described in the previous section for the reverse electron flow in ammonia oxidisers. But, the backwards running of complex III (Cyt c->UQH_2) is more difficult to explain.

We can propose 2 hypothesis to explain this backwards running (figure 16).

The first (figure 16-a) is easy to describe and is based on the following assumptions:

- at Qn site, the $UQ^{\cdot -}$ binding ability disappears. Driven by the $\Delta\psi$ forces, $UQ^{\cdot -}$ can then reach the Qp site, and the span UQ->bH becomes thermodynamically favourable.
- the electron passes from bH to bL driven by $\Delta\psi$ (which is the contrary of the normal path, but which is possible because ΔE of the reaction is close to $\Delta\psi$) However, that supposes an increase in $\Delta\psi$, what could occurs if H^+ (*i.e.* positives charges) are accumulated in the periplasm (increase of Δp).
- assuming potential of $UQ^{\cdot -}/UQH_2$ couple and Rieske protein are close, the reaction of step 1.1 (see section 2.3.1) is easily reversible, leading to UQH_2 formation.

It must be noted that this first description involves the transfer of $UQ^{\cdot -}$ in the membrane (not considered in the normal respiratory chain) and the suppression of the main assumption of the normal chain (*i.e.* the $UQ^{\cdot -}$ binding at Qn).

The second hypothesis consists in the complete reversibility of the mechanism involved in complex III (figure 16-b). This scheme is based on the following assumptions:

- at Qn site, the $UQ^{\cdot -}$ binding ability decreases, allowing the reaction :

$$UQ^{\cdot -} + b_{H-oxidised} \longrightarrow UQ + b_{H-reduced}$$

Assuming then that the $UQ^{\cdot -}$ binding gives a potential of the $UQ^{\cdot -}/UQ$ couple close to the b_H one, as a consequence, the potential of the $UQH_2/UQ^{\cdot -}$ couple will be close to the b_H one too, allowing the reaction:

$$UQH_2 + b_{H-oxidised} \longrightarrow 2H^+ + UQ^{\cdot -} + b_{H-reduced}$$

- the b_H - b_L electron transport is driven by Δy (see below).
- at Qp site, a binding ability of $UQ^{\cdot -}$ will drive the span b_L->$UQ^{\cdot -}$, and the $\frac{Cyt\ c_{oxidised}}{Cyt\ c_{reduced}}$ ratio (generated by NO_2^- oxidation) will probably force the span $UQ^{\cdot -}$->UQH_2 using 1 electron of reduced Cyt c.

This second hypothesis seems more difficult to justify on thermodynamic ground than the first one, but it implies only changes in the $UQ^{\cdot -}$ binding ability of the Qp and Qn site. That is the reason why it was chosen to describe the backwards running of complex III.

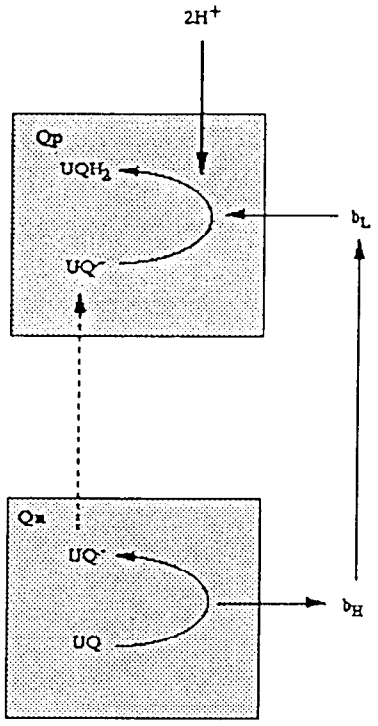

Figure 16-a

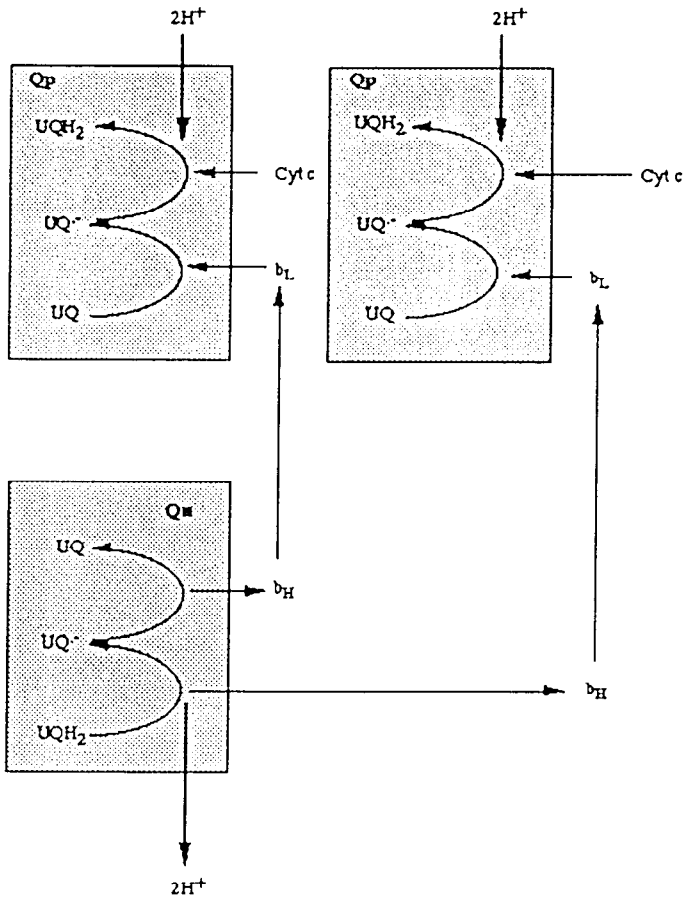

Figure 16-b

Figure 16 a-b : Two hypothesis for the reverse electron flow in complex III.

The complete stoichiometry (electron transport and its associated proton translocation) is reported in figure 17, and can be represented by the following group of reactions.

$$(NO_2^-, H^+) + H_2O + \text{Cyt } c_{ox} \longrightarrow (NO_3^-, H^+) + \text{Cyt } c_{red} + 2H^+$$

$$\text{Cyt } c_{red} + 8H^+_{out} + NAD \longrightarrow \text{Cyt } c_{ox} + NADH, H + 6H^+_{in} + H_2O$$

$$\text{Cyt } c_{red} + \frac{1}{2}O_2 + 4H^+_{in} \rightleftarrows \text{Cyt } c_{ox} + H_2O + 2H^+_{out}$$

$$3H^+_{out} + ADP + Pi \rightleftarrows 3H^+_{in} + ATP + H_2O$$

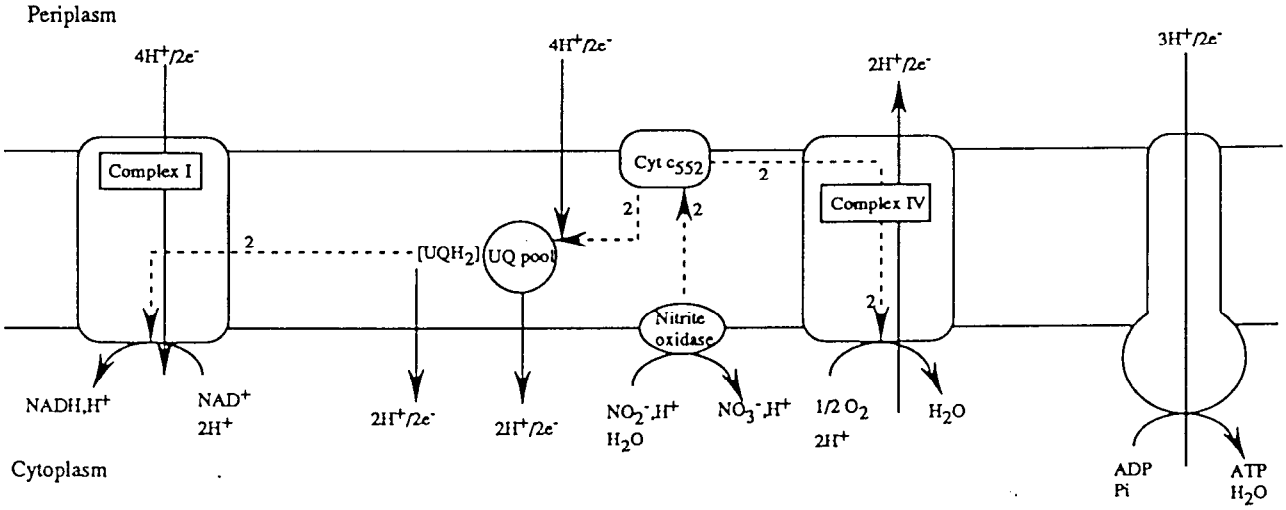

Figure 17: Proposed description of energetic metabolism of nitrite oxidisers

2.4 - Structured stoichiometric model of the nitrification phenomena

2.4.1 General features

The building of a structured stochiometric model of an organism requires to determine the different aspects of its metabolism, *i.e.* to establish the relations (or equations) which represent its catabolism, its anabolism, its maintenance term and its energetic metabolism.

In the case of nitrifying organisms (*Nitrosomonas* and *Nitrobacter*) the catabolism has not to be taken into account.

The equations representing the energy metabolism for the two organisms are presented above with their building hypothesis.

The maintenance term is generally considered as an ATP hydrolysis and is represented by the following equation:

$$ATP + H_2O \longrightarrow ADP + Pi$$

The anabolism involves all the metabolic pathways leading to the biomass biosynthesis (Amino-Acid biosynthesis pathways, lipids biosynthesis, tricarboxylic acids cycle, Calvin cycle, pentose pathway, etc...). A more detailed description of these pathways and their

equations will be given in a further technical note (TN 23.3). At the present time it must be only kept in mind that these pathways are commonly present in all organisms and can then be applied to nitrifiers.

The sum of all equations describing the metabolism is then a complex linear system of among 104 equations and 114 compounds. The resolution of such a system (metabolic matrix) requires to know and to fix several compounds (the percentage of protein in the biomass for example) or flows (absence of a pathway as the glyoxylate shunt for example).

2.4.2 Resolution of the metabolic matrix

The lack of information about the nitrifiers biomass has led to make assumption upon the biomass composition. A phylogenic relation has been established between *Nitrobacter winogradsky* and *Rhodopseudomonas palustris* (Seewaldt et al, 1982). However it can not be sufficient to state that the biomass composition of the two organisms is close. It was supposed that the known biomass composition of *Rhodospirillum rubrum* is the same as the nitrifiers biomass. This biomass (table 6) will be detailed in the TN 23.3.

Table 6: Biomass composition of *Rhodospirillum rubrum* .

Biomass composition (mass percentage)				
Proteins	lipids	Carbohydrates	RNA	DNA
65	12.2	16.9	4.9	1

Amino acids composition of proteins (molar percentage)									
glutamate	glutamine	proline	arginine	aspartate	asparagine	threonine	isoleucine	lysine	methionine
8.835	3.943	5.745	4.688	8.238	3.943	5.339	4.797	4.688	2.574
valine	leucine	alanine	serine	glycine	cysteine	phenylala.	tyrosyne	tryptophane	histidine
7.046	8.184	11.787	3.713	7.019	0	3.848	2.330	1.328	1.951

Lipids composition (molar percentage)					
Phosphatidic acid composition (ph)			Phospholipid composition		
palmitic acid	palmitoleic acid	vaccenic acid	Ph-ethanolamine	Ph-glycerol	diPh-glycerol
43.9	33.9	22.2	77.78	20.1	2.12

RNA	DNA CG%	Carbohydrates
same as E. coli	51% (from Nitrosomonas sp.)	Glu-6P polymer

Assuming the presence of α-ketoglutarate dehydrogenase is not compatible with a carbon economy based on CO_2 fixation by the requiring-energy RuBP carboxylase pathway, this part of the TCA cycle is suppressed. In the same way, the PEP carboxylase is supposed to be present, but the pathway of the glyoxylate shunt is supposed to be absent or inactive.

According to Prosser (1989), the maintenance represents 76% of the substrate consumption by Nitrosomonas (at an ammonium concentration of 1µgNH_4^+-N/ml) and 81% of the substrate consumption by Nitrobacter (at a nitrite concentration of 1µg NO_2^--N/ml).

From these assumptions, 2 global stoichiometric equations for Nitrosomonas and Nitrobacter can be established by solving the matrix of the biosynthesis pathway.

2.4.3 Stoichiometric equations

Nitrosomonas

$$CO_2 + 0.0089\ H_3PO_4 + 0.0035\ H_2SO_4 + 26.0166\ O_2 + 18.2606\ NH_3$$
$$\Downarrow$$
$$CH_{1.6147}O_{0.3906}N_{0.1994}S_{0.0035}P_{0.0089} + 18.0612\ (NO_2^-,H^+) + 8.5391 H_2O$$

Nitrobacter

$$CO_2 + 0.0089\ H_3PO_4 + 0.0035\ H_2SO_4 + 38.8496\ O_2$$
$$+ 79.8494\ (NO_2^-,H^+) + 0.1994\ NH_3 + 0.4914\ H_2O$$
$$\Downarrow$$
$$CH_{1.6147}O_{0.3906}N_{0.1994}S_{0.0035}P_{0.0089} + 79.8494\ (NO_3^-,H^+)$$

Nitrification with no production of nitrite

A nitrification which completely exhaust nitrite can be represented by coupling these two previous equations. The following stoichiometry is the result of this coupling:

$$CO_2 + 0.0089\ H_3PO_4 + 0.0035\ H_2SO_4 + 28.3838\ O_2 + 14.9289\ NH_3$$
$$\Downarrow$$
$$CH_{1.6147}O_{0.3906}N_{0.1994}S_{0.0035}P_{0.0089} + 14.7295\ (NO_3^-,H^+) + 6.8733\ H_2O$$

The biomass produced by this stoichiometry represent the sum of the biomass of *Nitrosomonas* and *Nitrobacter* and is composed of 81% of *Nitrosomonas* and 19% of *Nitrobacter*.

The main results deduced from the stoichiometry (and of the solving of the metabolic fluxes) are reported in table 7.

Table 7: Yields of the nitrification

	Nitrosomonas	*Nitrobacter*	Nitrification
N oxidised / CO_2 assimilated (mol/mol)	18.061	79.849	14.729
CO_2 assimilated / N oxidised (mol/mol)	0.0554	0.0125	0.0679
N oxidised / CO_2 assimilated (mg/mg)	46.746	74.794	38.123
Biomass formed / N oxidised (g/mol)	1.276	0.288	1.564
O_2 / N oxidised (mol/mol)	1.441	0.486	1.927
CO_2 assimilated / O_2 (mol/mol)	0.038	0.0257	0.035
CO_2 assimilated by Calvin / CO_2 assimilated	92.65%	92.65%	-
ATP for maintenance / ATP produced	91.57%	93.60%	-
Electrons in the reverse electron transport chain	23.81%	2.69%	-

These results can be compared with the experimental yields reported in tables 1 and 2. It can be noted that the values deduced from the stoichiometry are quite close to the experimental ones. The O_2 / N oxidised ratios are close to those generally used to describe the nitrification by

kinetic model (see section 1) and which are respectively 1.5 and 0.5 for *Nitrosomonas* and *Nitrobacter*.

But it must be outlined that only a few part (24% and 3%) of the electrons released by the N-oxidation run backward the respiratory chain, while the other part reaches the terminal oxidase, allowing ATP synthesis. The main part of the ATP produced appears to be hydrolysed for maintenance (over 90%). It is the consequence of the assumption which states that 76% of NH_3 and 81% of NO_2^- are oxidised for maintenance.

2.4.4 Origin of the apparent high value of maintenance

As mentioned above, the metabolism of an organism can be divided in 4 parts: anabolism, catabolism, maintenance and energy metabolism. The equations characterising each of them can be established for *Nitrosomonas*.

Anabolism (equation deduced from the solving of the metabolic matrix with no maintenance)

$$CO_2 + 0.0089\ H_3PO_4 + 0.0035\ H_2SO_4 + 2.9468\ NTP + 1.2879\ H_2O + 0.1994\ NH_3 + 2.1502\ CofH_2$$
$$\Downarrow$$
$$CH_{1.6147}O_{0.3906}N_{0.1994}S_{0.0035}P_{0.0089} + 2.9468\ (NDP + Pi) + 2.1502\ Cof$$

Maintenance

$$ATP + H_2O \longrightarrow ADP + Pi$$

Energy metabolism

$$NH_3 + \frac{5}{4}O_2 + 4H^+_{in} + \frac{1}{2}UQ \longrightarrow 4H^+_{out} + (NO_2^-, H^+) + \frac{1}{2}UQH_2 + \frac{1}{2}H_2O$$

$$UQH_2 + 6H^+_{in} + \frac{1}{2}O_2 \longrightarrow UQ + 6H^+_{out} + H_2O$$

$$NAD^+ + UQH_2 + 4H^+_{out} \rightleftarrows NADH,H^+ + UQ + 4H^+_{in}$$

$$3H^+_{out} + ADP + Pi \rightleftarrows 3H^+_{in} + ATP + H_2O$$

It must be kept in mind that these equations (especially for energetic metabolism) represent the theoretical stoichiometry of the reactions. Moreover, the coupling between all the reactions has been supposed to be equal to 1, in order to solve the metabolic matrix.

But in vivo, it exists energy losses. For the respiration, for example, the theoretical P/O ratio for the transport of 2 electrons from $NADH,H^+$ to the terminal oxidase is 10/3 (3.33), but the P/O usually observed in vivo is 1.7.

It can be noted, for *Nitrosomonas*, if no maintenance is assumed, and if the coupling is supposed to be perfect (*i.e.* equal to 1), that the $\frac{N_{oxidised}}{CO_2}$ ratio is 4.335 (18.061 with the maintenance assumption).

Assuming a coupling factor of 0.6 for the H+ transfer across the membrane, and assuming that 60% of the ATP synthetised is hydrolysed by the maintenance reaction, this $\frac{N_{oxidised}}{CO_2}$ ratio reaches 14.03. The results obtained for this stoichiometry are already in the range of experimental values, and the apparent maintenance value is 71% of the NH_3 oxidised.

The same assumptions made for *Nitrobacter* give similar results:

$\frac{N_{oxidised}}{CO_2}$=54.35

Maintenance=72.09% of NO_2^- oxidised

2.4.5 Biomass composition

The analysis of a biomass sample of an axenic fed-batch coculture of *Nitrosomonas europae* and *Nitrobacter winogradsky* (Forler, 1994) have given the following C-molar biomass composition:

$CH_{1.9168}O_{0.4055}N_{0.1553}S_{0.0034}P_{0.0072}$

In the present calculations, the biomass composition has been considered to be identical to the *Rhodospirillum rubrum* composition which leads to $CH_{1.6147}O_{0.3906}N_{0.1994}S_{0.0035}P_{0.0089}$.

It must be noted that the biomass C-molar composition supposed for the stoichiometry building is significantly different of the experimental one, mainly for the H and N ratios. If we suppose that the macroelements (proteins, lipids...) elemental composition has been correctly estimated, it must be concluded that the relative weight fractions of these macroelements are significantly different in the N-oxidisers cells. Therefore, these fractions have to be experimentally determined for further studies.

However, in order to achieve the present calculations, it has been necessary to keep to *Rhodospirillum rubrum* composition.

Considering N is mainly provided by proteins, the experimental N/C ratio obtained, supposes a protein composition less than 65% (probably near 50%). It can be supposed that the organism accumulates reserve polymers (poly β-hydroxybutyrate, glycogen and polyphosphate in the case of Nitrobacter, Hooper, 1987).

2.4.6 Analysis of the H^+/O ratio of *Nitrosomonas*

The generation of proton gradient during ammonia and hydroxylamine oxidation by Nitrosomonas has been studied. The proton gradient, extrapolated to the upper limit of H^+/O, was 3.4 for NH_3 and 4.4 for NH_2OH (Wood, 1986).

From the energetic metabolism of Nitrosomonas, proposed in figure 14, the following H^+/O ratio can be deduced:

H^+/O=3.33 from NH3 oxidation

H^+/O=6 from NH_2OH oxidation

The ratio deduced from our proposed description of the Nitrosomonas energy metabolism is then close to the extrapolated one for ammonia oxidation, but very different for NH_2OH oxidation.

Assuming the span HAO -> UQ pool is unfavourable if there is no ammonia oxidation (*i.e.* there is no electron transfer from UQ pool to AMO), it can be supposed that all electron released by NH_2OH oxidation reach the cytochrome c_{552} (instead of the partition between UQ pool and cytochrome c_{552}). This assumption leads to an H^+/O of 4.5, close to the extrapolated one.

2.5 - Analysis of the oxygen gas-liquid limitation during nitrification.

Several parameters drive the nitrification efficiency. The main of them are pH (Laudelout et al., 1976), the oxygen limitation, the NH_3 limitation (and inhibition), the NO_2^- limitation and inhibition (Hunik et al., 1994). The limitations can occur through transfer limitations or input limitations.

Studies have been driven for transfer limitation (liquid-solid transfer and diffusion limitation) in K-carrageenan gel beads (Hunik et al., 1994) or in biocatalyst particule (Hooijman et al., 1990), implying different kinetic models. It must be noted that such limitations will probably not occur in the pilot fixed bed reactor developed for the nitrifying MELiSSA compartment. The polystyrene beads (Biostyr), chosen to fix the organisms, allow the growth only on the surface of the beads (micro-organisms can growth inside the gel beads), and thus, the transfer limitations inside the beads have not to be studied.

The aim of this section is to present a simple relation allowing the estimation of one of the parameter for the nitrifying reactors: the $k_La|_{O_2}$ value, which drive the gas-liquid oxygen transfer limitation phenomenum (the role and the importance of the k_La.has been explained in TN 23.1).

The profile of the oxygen concentration in the bulk can be defined as a function of the time by the following kinetic relation:

$$\frac{dC_{O_2}}{dt} = k_La|_{O_2} \cdot \left(C^*_{O_2} - C_{O_2}\right) + r_{O_2}$$

where: C_{O2} is the oxygen concentration in the liquid phase
C_{O2}^* is the oxygen concentration at saturation in the liquid phase
r_{O2} is the production rate of oxygen (positive if O_2 is produced and negative if O_2 is consumed by the microorganism)

Assuming the oxygen limitation occur when

$$\frac{dC_{O_2}}{dt} = 0$$

and

$$C_{O_2} = 0$$

then, the relation becomes

$$k_La|_{O_2} \cdot C^*_{O_2} = -r_{O_2}$$

r_{O2} is the production rate of oxygen. It can be expressed as a function of the biomass production rate of *Nitrosomonas* (noted r_X^{Ns}) and of *Nitrobacter* (noted r_X^{Nb}):

$$r_{O_2} = - Y_{O_2/X}^{Ns} . r_X^{Ns} - Y_{O_2/X}^{Nb} . r_X^{Nb}$$

where $Y_{O_2/X}^{microorganism}$ is the yield of the moles of oxygen consumed by gram of biomass for a microorganism. This yield can be deduced from the stoichiometry.

Assuming that there is no other limitation for the growth of the micro-organisms (NH_3 limitation, CO_2 limitation, NO_2^- limitation ...) and that there is no accumulation of the intermediate NO_2^- between the two organisms, then the production rate of nitrite by *Nitrosomonas* is equal to the consumption rate of nitrite by *Nitrobacter* . Because of the consumption rate of nitrite by *Nitrobacter* is equal to the production rate of nitrate, the following relation can be written:

$$r_X^{Ns} . Y_{NO_2/X}^{Ns} = r_X^{Nb} . Y_{NO_3/X}^{Nb}$$

then

$$r_X^{Nb} = \frac{Y_{NO_2/X}^{Ns}}{Y_{NO_3/X}^{Nb}} . r_X^{Ns}$$

where $Y_{NO_2/X}^{Ns}$ and $Y_{NO_3/X}^{Nb}$ are respectively the yield of moles of nitrite produced by gram of *Nitrosomonas* and the yield of moles of nitrate produced by gram of *Nitrobacter* .

The oxygen transfer limitation relation becomes:

$$k_L a|_{O_2} . C_{O_2}^* = \left[Y_{O_2/X}^{Ns} + Y_{O_2/X}^{Nb} . \frac{Y_{NO_2/X}^{Ns}}{Y_{NO_3/X}^{Nb}} \right] . r_X^{Ns}$$

Considering the complete stoichiometry for the nitrification (deduced from the equations of *Nitrosomonas* and *Nitrobacter*), an other expression for r_{O2} can be proposed:

$$r_{O_2} = - Y_{O_2/X} . r_X$$

where r_X is the biomass production rate (*Nitrosomonas* and *Nitrobacter*) of the nitrification.

The oxygen transfer limitation relation then becomes:

$$k_L a|_{O_2} . C_{O_2}^* = Y_{O_2/X} . r_X$$

By the same way, r_{O2} can be expressed as a function of the other production rates, as r_{NO3} (nitrite production rate in moles NO_3^- by gram of total biomass produced), and the oxygen transfer limitation relation becomes:

$$k_L a|_{O_2} . C_{O_2}^* = Y_{O_2/NO_3} . r_{NO_3}$$

These relations determine the minimal $k_La|_{O_2}$ values necessary to run the nitrification without oxygen limitation assuming a fixed r_X (or r_{NO3}).These relations are reported in figures 18 and 19, and the values of the parameters required to solve the relations, reported in table 8, are calculated from the coefficients of stoichiometric equations. It must be kept in mind that the $k_La|_{O_2}$ values determined by these relations are not taken into account the other limitations (NH_3, NO_2^-, CO_2 or pH), or inhibitions (O_2, NO_2^-), which can accur.

Table 8: Parameters of the oxygen transfer limitation relations.

Parameter	Value	Units
$Y^{Ns}_{O_2/X}$	1.1292	mol O_2/ g biomass *Nitrosomonas*
$Y^{Nb}_{O_2/X}$	1.6862	mol O_2/ g biomass *Nitrobacter*
$Y^{Ns}_{NO_2/X}$	0.7839	mol NO_2^-/ g biomass *Nitrosomonas*
$Y^{Nb}_{NO_3/X}$	3.4657	mol NO_3^-/ g biomass *Nitrobacter*
$Y_{O_2/X}$	1.2319	mol O_2/ g biomass *Nitrosomonas* + *Nitrobacter*
Y_{O_2/NO_3}	1.9270	mol NO_3^-/ g biomass *Nitrosomonas* + *Nitrobacter*
$C^*_{O_2}$	$2.7218\ 10^{-4}$	mol/l

Y are deduced from the stoichiometries (see table 7)

$C^*_{O_2}$ is calculed for an air input at 25°C by using the relation developed in TN 17.1

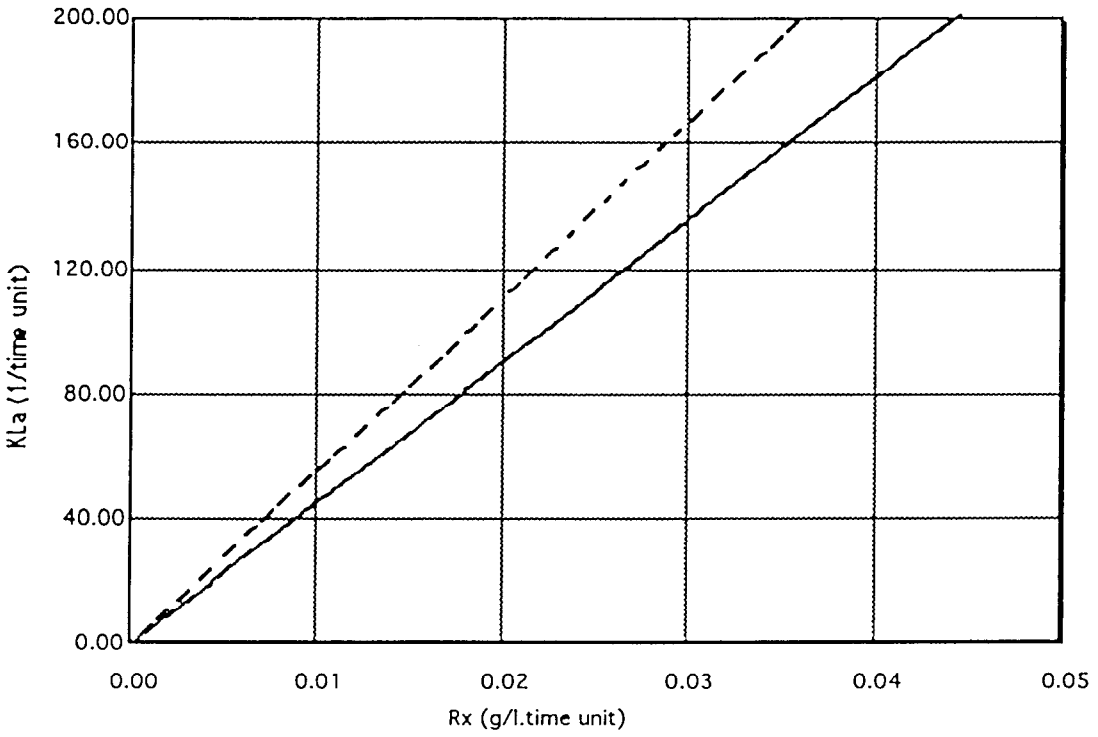

Figure 18: $k_La|_{O_2}$ as a function of r_X^{Ns} (dashed line) and r_X.

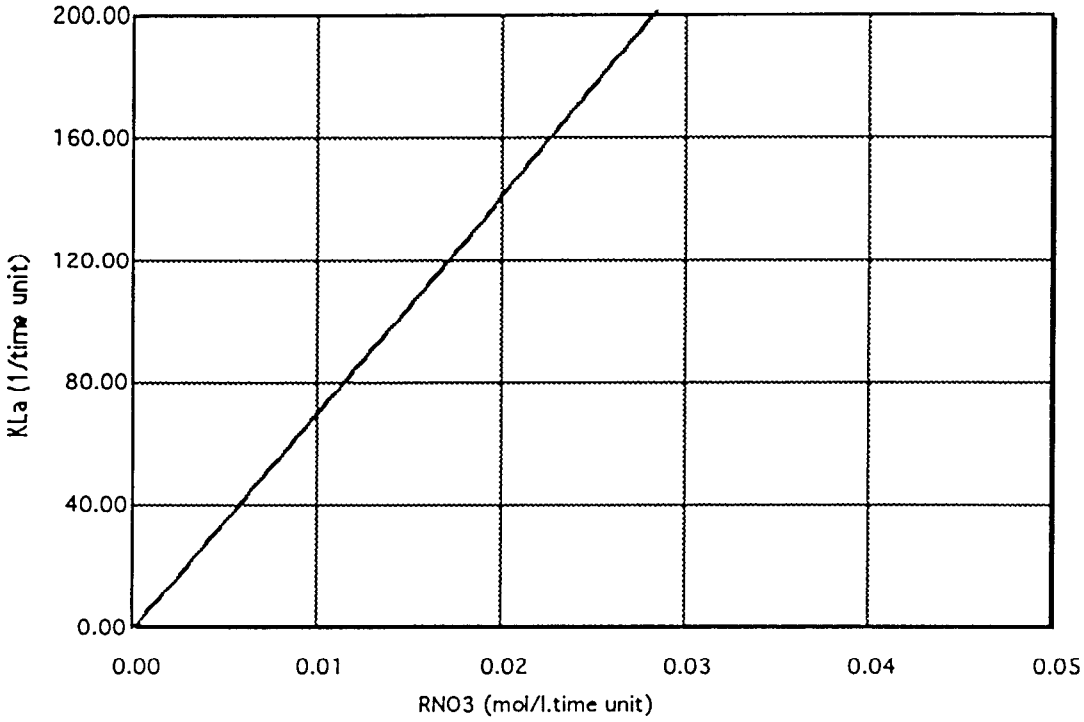

Figure 19: $k_L a|_{O_2}$ as a function of r_{NO3}.

CONCLUSION

A theoritical description of the respiratory chain of Nitrosomonas and Nitrobacter, involving the links between electrons transport, protons translocation and N-oxidation reactions, has been made. From these descriptions, which include assumptions for the reverse electrons transport chain, the stoichiometries of the energy metabolism of the two organisms can be established.

By coupling these stoichiometries to the stoichiometries which represent the anabolism and the maintenance, stoichiometric equations can then be built to represent the N-oxidations by *Nitrosomonas* and *Nitrobacter*.

One of the informations used to establish the stoichiometry of the two organisms is the maintenance. It appears that the apparent high value of the maintenance (*i.e.* more of 90% of ATP synthetised is hydrolysed by the maintenance reaction), mainly results of the coupling factors between protons translocation, ATP synthesis and electrons transport in the respiratory chain. These coupling factors are already present in all organisms., but in the case of nitrifiers organisms, a high amount of energy (Δp, reduced power and ATP) is required for CO_2 fixation and for the reverse electron flow. The relative weight of the coupling factors in the energy metabolism of nitrifiers is then more important than for the other organisms and explains then the apparent high value of the maintenance. Moreover the energy metabolism of nitrifiers is linked to their N-oxidation abilities, thus the coupling factors appear to be important in the description of the N-oxidation reactions.

The biomass defined in the stoichiometries is different of the experimental one. The experimental N/C ratio supposes a protein composition near 50% (mass percentage of the dry biomass), instead of the 65% used in the stoichiometry. It must be kept in mind that the biomass composition used to built the stoichiometries is taken from Rs rubrum. That can explain why the stoichiometric CHONSP biomass and the experimental one are different. The difference would be reduced if, at least, a mean macroelement composition (% proteins, % lipids, % carbohydrates) was defined.

The oxygen transfer limitation has been studied through a relation giving the $k_La|_{O_2}$ value necessary to run the nitrification without oxygen limitation. The $k_La|_{O_2}$ is an important parameter for the biological reactions involving oxygen, and is one of the parameters required in the building of a kinetic model.

Instead of the unclear definition of the maintenance, stoichiometries for the nitrification have been established. These stoichiometries will be the base for the development of the next step in the study of the nitrifying compartment modelling: the building of a kinetic model.

REFERENCES

Aleem M.I.H., Hoch G.E. and Varner J.E. (1965)
Water as the source of oxidizing and reducing power in bacterial chemosynthesis. Proceedings of the National Academy of Sciences. USA. 54. pp 869-873.

Aleem M.I.H. and SewellD.L. (1984)
Oxidoreductase system in Nitrobacter agilis .Microbial chemoautotrophy. Strohl W.R. and Tuovinen O.H. editors. pp. 185-210.

Andersson K.K. and Hoopper A.B. (1983)
O_2 and H_2O are each the source of one O in NO_2: ^{15}N-NMR evidence. FEBS Letters 164. pp.236-239.

Bock E., Koop H.P., Ahtlers B. and Harms H. (1991)
Oxydation of inorganic nitrogen compounds as energy source. The prokaryotes (2nd ed.) Balows A., Trüper H.G., Dworkins M., Hender W. and Scheifer K.H. Springer Verlag. pp. 414-430.

Bock E., Koop H.P., Harms H. and Ahtlers B. (1991)
The biochemistery of nitrifying organisms. Variation in autotrophic life. Shively J.M. and Barton L.L. editors. Academic Press.

Fenckel T. and Blackburn T.H. (1979)
Bacteria and mineral cycling. Institute of Ecology and genetics. Aarhus, Denmark. Academic Press. pp. 111-118.

Forler C. (1994)
MELiSSA. Development of a fixed bed pilot reactor for a continuous axenic coculture of *Nitrosomonas europaea* and *Nitrobacter winogradsky*. ESA-X-997

Geraats S.G.M., Hooijmans C.M., Van Neil E.W.J., Robertson L.A. Heijnen J.J. and Luyben K.Ch.A.M. (1990)
The use of a metabolically structured model in the study of growth, nitrification and denitrification by *Thiosphaera pantotropha*. Biotech. Bioeng. Vol. 36. pp. 921-930.

Glover H.E. (1985)
Archives of microbiology. 142. p. 45.

Gunsalus I.C. and Stanier R.Y. (1962)
The bacteria-a treatise on structure and function. Academic press. 3. pp.2-3.

Hooijmans C.M, Geraats S.G.M., Van Neil E.W.J., Robertson L.A. Heijnen J.J. and Luyben K.Ch.A.M. (1990)
Determination of growth and coupled Nitrification/Denitrification by Immobilized *Thiosphaera pantotropha* using measurement and modeling of oxygen profiles. Biotech. Bioeng. Vol. 36. pp. 931-939.

Hooper A.B. (1987)
Biochemistry of the nitrifying lithoautotrophic bacteria. In Autotrophic bacteria. FEMS Science Tech. Publisher (Ed.). pp.239-265.

Hunik J.H., Bos C.G., Van den Hoogen M.P., De Gooijer C.D. and Tramper J. (1994)
Co-immobilized *Nitrosomonas europaea* and *Nitrobacter agilis* cells: validation of a dynamic model for simultaneous substrate conversion and growth in K-carrageenan gel beads. Biotech. Bioeng. Vol 43. pp. 1153-1163.

Kelly D.P. (1978)
In "Companion to microbiology". Bull A.T. and Meadow P.M. editors. pp. 363-386.

Laudelout H., Lambert R. et Pham M. (1976)
Influence du pH et de la P_{O2} sur la nitrification. Ann. Microbiol. 127. pp. 367-382.

Mitchell P. and Moyle J.(1967)
Respiration-driven protonb translocation in rat liver mitochondria. Biochem. J. N°104. pp. 588-600

Nicholls D.G. and Ferguson S. (1992)
Bioenergetics 2. Academic Press.

Noorman H. (1991)
Methodology on monitoring and modelling of microbial metabolism. Thesis of the Delft university of technology. Netherlands.

Olson T.C. and Hooper A.B. (1983)
FEMS Microbiol. Lett. 19. pp. 407.412.

Prosser J.I. (1989)
Autotrophic nitrification in bacteria. Advances in microbial physiology. Vol. 30. Academic Press. pp 125-177.

Rottenberg H. and Gutman M. (1977)
Control of the rate of reverse electron transport in submitochondrial particles by the free energy. Biochemistry. Vol 16. N°14. pp. 3220-3226.

Seewaldt E., Schleifer K., BVock E. and Stackerbradt E. (1982)
The close phylogenetic relationship of *Nitrobacter* and *Rhodopseudomonas palustris*. Acta Microbiol. 131, pp.287-290.

Suzuki I., Dular U. and Kwok S.C. (1974)
Journal of bacteriology. 120. p.556.

Tsang D.C.Y. and Susuki I. (1982)
Can. J. Biochem. 60. pp. 1018-1024.

Wood P.M. (1986)
Nitrification as a bacterial energy source. In"Nitrification". Prosser J.I. editor.Special publication of the society for general microbiology. Vol. 20. IRL Press. pp.39-62.